

# Repair of alveolar cleft bone defects by bone collagen particles combined with human umbilical cord mesenchymal stem cells in rabbit

**Xue-Cheng Sun**

National Research Institute for Family Planning <https://orcid.org/0000-0002-1689-2627>

**Hu Wang**

Reproductive and Genetic Center of National Research Institute for Family Planning

**Jian-Hui Li**

Reproductive and Genetic Center of National Research Institute for Family Planning

**Dan Zhang**

Reproductive and Genetic Center of National Research Institute for Family Planning

**Xu Ma**

Reproductive and Genetic Center of National Research Institute for Family Planning

**Hong-Fei Xia** (✉ [hongfeixia@126.com](mailto:hongfeixia@126.com))

Reproductive and Genetic Center of National Research Institute for Family Planning

---

## Research

**Keywords:** alveolar cleft, Bone collagen particles, HUC-MSCs (human umbilical cord mesenchymal stem cells), micro-focus computerized tomography (micro-CT)

**Posted Date:** April 22nd, 2020

**DOI:** <https://doi.org/10.21203/rs.2.22764/v3>

**License:**  This work is licensed under a Creative Commons Attribution 4.0 International License.

[Read Full License](#)

---

**Version of Record:** A version of this preprint was published on August 3rd, 2020. See the published version at <https://doi.org/10.1186/s12938-020-00800-4>.

# Abstract

**Background:** Alveolar cleft is a kind of cleft lip and palate, which seriously affects the physical and mental health of patients. In this study a model of the alveolar cleft phenotype was established in rabbits to evaluate the effect of bone collagen particles combined with human umbilical cord mesenchymal stem cells (HUC-MSCs) on the repair of alveolar cleft bone defects.

**Methods :** The model of alveolar clefts in rabbits was established by removing the incisors on the left side of the upper jaw. Bone collagen particles combined with hUC-MSCs were implanted in the defect area. Blood biochemical analysis was performed after 3 months. Skull tissues were harvested for gross observation, and micro-focus computerized tomography (micro-CT) analysis. Tissues were harvested for histological and immunohistochemical staining. The experiments were repeated 6 months after surgery.

**Results:** The bone collagen particles and HUC-MSCs have good biological safety. In addition, both can promote the regeneration of incisor. Bone collagen particles combined with hUC-MSCs were much better than those used alone in inducing bone repair and regeneration.

**Conclusions:** The method of HUC-MSCs combined with bone collagen particle material to fill a bone defect site is simple, rapid and suitable for the treatment of alveolar cleft bone defects.

## Background

Alveolar cleft is commonly in clinics, which not only affects the normal eruption of teeth and the development of the jaws, but also affects the physical and mental health of patients. Therefore, it is very important to establish an animal model of alveolar clefts that is similar to human alveolar cleft disease and can be repeated. This method can provide a theoretical basis for the occurrence and development of the disease, and also provide a good scientific research foundation for the repair of alveolar clefts.

The most commonly used model animals are primates [1,2], sheep[3], canine animals[4], felids[5], rodents and rabbits[6,7]. Rabbits have the advantages of short growth cycle, easy feeding and low cost. Moreover, compared with other animals, rabbits are of moderate size, gentle temperament and easier to operate. Studies in our laboratory have also proved that rabbits can be used to establish animal models of the alveolar cleft [8]. Therefore, rabbits were selected as experimental animals to establish the animal model of alveolar clefts.

Alveolar cleft caused only by facial muscles can be corrected or repaired by surgical suture, but there is still no effective treatment for alveolar clefts caused by bone defect. At present, the treatment methods of alveolar clefts can be divided into distraction osteogenesis and bone grafting.

Traction osteogenesis refers to the technology of bone correction or repair by applying physical traction force in a specific direction and frequency to partially or completely detached biological tissue so that the gap is gradually replaced by new bone. Binquer et al. used traction osteogenesis to correct alveolar cleft

[9]. Although this method avoids the immunogenicity of the foreign implanted tissue, the procedure is complicated, requires a long treatment period, and requires two surgeries to place and remove the retractor. Still not a good treatment.

Bone materials commonly used in bone grafting to include autogenous bone, allogeneic bone, allogeneic bone and tissue-engineered bone. Boyne et al. have repaired oronasal fistulas by inserting a small amount of cancellous bone from the autogenous ilium into the fractures [10]. This method is considered to be the gold standard for the clinical repair of alveolar clefts [11,12]. Nevertheless, autologous bone grafts are bound to cause donor trauma and deformity, which an ideal repair should avoid. Nique et al. once used allograft bones to treat alveolar clefts, and postoperative imaging showed that the tooth successfully erupted and grew into the graft bone, but this process required a long time [13]. El Deeb et al. fill hydroxyapatite in the crack of the alveolar clefts and found no tooth eruption [14]. Allogeneic bone allograft or artificial bone, although can avoid donor-site deformity, but there is a risk of immune rejection and transmission of disease. With the development of tissue engineering technology, the application of tissue engineering bones to repair alveolar fractures are no longer a problem. Currently, the most widely used scaffold materials are collagen[15],hydroxyapatite[16],calcium sulfate[17], calcium phosphate cement[18] , Bioactive glass[19] and so on . Because of the complex structure and function as bone tissue, it is difficult for a single material to meet the demand. It is commonly used to repair alveolar clefts by combining scaffold materials with factors or stem cells that induce bone regeneration. Compared with factors, stem cells have the advantages of low cost and easy access. Common stem cells are bone marrow mesenchymal stem cells [20], umbilical cord mesenchymal stem cells [21.22], embryonic stem cells and so on. Compared with stem cells derived from bone marrow, stem cells derived from umbilical cord have the advantages of low immunogenicity, rapid proliferation, wide availability and low ethical concerns [22,23]. Chronic spinal cord injury to dogs has been treated with hUC-MSCs combined with collagen scaffolds [24].

In this study, bone collagen granules prepared by decellularization and degreasing of bovine cancellous bone were used as scaffold materials. The main ingredients are collagen and hydroxyapatite. It not only preserves its natural three-dimensional porous structure, but also reduces its immunogenicity. On this basis, composite human umbilical cord derived mesenchymal stem cells were used to repair alveolar fissures.

The purpose of this study was to investigate the feasibility and effectiveness of bone collagen particles inoculated with hUC-MSCs in the rabbit model of alveolar clefts. The results indicate that hUC-MSCs combined with bone collagen particles may be a reliable alternative therapy for the repair of alveolar bone defects.

## Results

### Blood analysis

Blood routine (Table 1&4), liver function (Table 2&5), renal function (Table 3&6) and BGP of each group were measured at 3 and 6 months after the surgery, and the values of each group were compared with those of the normal group. The blood routine results showed that NEUT content increased and LYM content decreased in the control group at 3 months, and they all tended to be normal at 6 months. The content of CRP, EO and NEUT in the material group increased at 3 months, while the content of the LYM decreased, and all of them tended to be normal at 6 months. CRP contents in MSCs group decreased from 6 months, and other indicators showed no significant abnormality. Liver function results showed that ALT and AST levels in the control group were higher than those in the normal group at 3 and 6 months. The content of ALT and AST in the material group was higher than that in the normal group at 3 months and normal at 6 months. No significant abnormalities were found in the MSCs group. Renal function results showed that CR levels in the control group, the materials group and the MSCs group increased significantly at 3 months and tended to normal at 6 months. The BUN content of the control group and MSCs group increased significantly at 3 months and tended to be normal at 6 months.

BGP results showed that at 3 months, the control group was lower than the normal group, while the materials group and the MSCs group were not significantly different from the normal group (Figure 2a). At 6 months, the content of BGP in the material group decreased, while that in the MSCs group increased even higher than that in the normal group (Figure 2b). In the normal group, the BGP content was stable at about 30ug/l in both periods. The content of BGP in the control group was slightly lower than that in the normal group at 3 months and tended to be normal at 6 months. We speculate that bone absorbency increases after bone removal, which tends to be stable over time. The content of BGP in the material group tended to be normal at 3 months and lower at 6 months. Due to the high bone conversion rate of collagen scaffold materials, when bone absorption is greater than bone formation, it will lead to a decrease in BGP content. The BGP content of MSCs group was slightly higher than that of normal group due to the continuous effect of bone formation. We hypothesized that hUC-MSCs could prolong bone repair time. This indicated that neither bone collagen granule material nor hUC-MSCs were toxic, and that hUC-MSCs could reduce inflammatory reactivity.

## Imaging analysis

**General observation (Figure 3).** The appearance of the skull was observed from both vertical and horizontal angles, with the surgical position in the red box. From a vertical point of view, asymmetry of the left and right maxillary bone was observed in both the control group and the material group, while no significant asymmetry was observed in the MSCs group. From a horizontal point of view, the area of new bone in both the material group and the MSCs group was higher at 6 months than at 3 months. The percentage of bone trabeculae and the percentage of bone mineral density of new bone in the material group and the MSCs group increased significantly, while the surgical location of the control group did not change significantly into the two periods.

**Micro-CT imaging.** The internal images of the normal side and the operative side of each group were compared to 3 or 6 months for preliminary analysis (Figure 4 A&B). The red box is the surgical site.

Accurate analysis of bone density and percentage of trabecular bone in each group (Figure 4 C). Internal images of both angles showed no significant repair of the operative side in the control group during the two periods. A small amount of new bone tissue was found on the surgical side of the material group. A significant amount of new bone tissue was found on the surgical side of the MSCs group 6 months after surgery. The results showed that the percentage of bone trabeculae was the highest in the MSCs group, followed by the material group and the lowest in the control group (Figure 4 Ca& Cc). Bone mineral density (BMD) of control group, material group and MSCs group was not significantly different at 3 months (Figure 4 Cb). BMD of MSCs group was significantly higher than that of the other two groups at 6 months (Figure 4 Cd). Therefore, the osteogenic ability of bone collagen particles combined with hUC-MSCs was significantly better than that of bone collagen particles alone.

## Histological analysis

**HE staining:** HE staining showed that the normal incisor bone was a uniform bone matrix (Figure 5a1&e1). The bone defect area without any implanted material showed no new bone formation at both periods, only a few scattered bits of bone (Figure 5b1&f1). Three months after bone collagen particles implantation alone, a large number of bone fibers and a small amount of bone marrow and trabeculae were seen in the bone defect area (Figure 5c1). After 6 months, there were still only a small amount of bone marrow and trabeculae in the bone defect area, and the rest were cavitation structures (Figure 5g1). Three months after the implantation of bone collagen particles in combination with hUC-MSCs, a large number of trabeculae and fibrous tissues appeared in the bone defect area (Figure 5d1). After 6 months, a large new bone formation was evident in the bone defect area (Figure 5h1).

**Sirius red staining:** Type 1 collagen can be stained bright orange by Sirius red staining. Sirius red staining results showed that collagen type 1 was high and evenly distributed in the normal incisor bone (Figure 6 Aa&e). In the control group, only a minimal amount of type 1 collagen was present in the scattered bones (Figure 6 Ab &f). Only a small amount of collagen type 1 can be seen in the bone defect area after the bone collagen particles were implanted (Figure 6 Ac &g). After the implantation of bone collagen particles combined with hUC-MSCs, a large amount of collagen type 1 appeared in the bone defect area (Figure 6 Ad &h). Compared with the normal group, the content of collagen type 1 in each group was statistically different at 3 months (Figure 6B) and 6 months (Figure 6c) postoperatively.

**PAS staining** PAS staining can stain chondrocytes dark purple or crimson. The results of PAS staining showed that the normal incisor bone was a uniform bone matrix with no chondrocellular structure (Figure 7a&e). The structure of bone defect in the control group was the cavitation structure, and chondrocyte structure was not observed (Figure 7b&f). A small amount of dark purple or crimson areas can be seen in the bone defect area after implantation of bone collagen particles alone, which indicates the presence of a small amount of chondrocytes (Figure 7c&g). After the implantation of bone collagen particles in combination with hUC-MSCs, a large number of dark purple or crimson areas appeared in the bone defect area, which indicates the presence of a large number of chondrocytes (Figure 7d & h).

**ALP** ALP staining can indirectly stain osteoblasts black. ALP staining showed the normal incisor bone was a uniform bone matrix with no osteoblasts structure (Figure 8 a&e). The structure of bone defect in the control group was the cavitation structure, and osteoblasts structure was not observed (Figure 8 b&f). There are a lot of black spots in the bone defect area of material group and MSCs group at 3 months (Figure 8 c&d), 6 months reduced numbers of black spot (Figure 8 g&h), which indicates the change trend of osteoblasts existed from high to low. **IHC (BMP-2)** It has been reported that BMP-2 play pivotal roles in bone formation. Overexpression of BMP-2 is involved in regulating the formation and remodeling of mineralized tissue [25]. Immunohistochemical results showed that the positive rate of bmp-2 was very low in the normal group and the control group (Figure 9a, b, e&f). In the materials group and the MSCs group, BMP-2 was mainly expressed in osteocytes and osteoclasts at the edge of trabecular bone (Figure 9c, d, g&h). The expression level of BMP-2 in the material group and the MSCs group at 3 months after surgery was significantly higher than that at 6 months after surgery. The expression level of BMP-2 was the highest in MSCs group. The results showed that the ability of active collagen particles combined with hUC-MSCs to induce the generation of BMP-2 was better than that of bone collagen particles alone.

### **Proliferation and apoptosis analysis**

Ki67 (Figure 10B) and TUNEL (Figure 10A) methods were used to detect cell proliferation and apoptosis in each group at 3 and 6 months after surgery. TUNEL assay (Figure 10C1) showed that the positive rate of the control group was similar to that of the normal group of 3 months after surgery. The positive rate of the material group was lower than that of the normal group. The positive rate of MSCs group was significantly higher than that of normal group. The immunohistochemical test results of Ki67 (Figure 10C2) showed that the positive rate of the control group and the material group was significantly lower than that of the normal group at 3 months after the surgery. The positive rate of the MSCs group was similar to that of the normal group. At 6 months after the surgery, there was no significant change in the positive rate of the control group, which was still lower than that of the normal group. The positive rate of the material group increased obviously, but did not exceed that of the normal group. The positive rate of the MSCs group was still close to that of the normal group.

## **Discussion**

HUC-MSCs were taken from neonatal umbilical cords. Therefore, it has the advantages of abundant source, low cost, no harm to donors. The neonatal umbilical cords are medical waste, which is less ethical controversial than other source tissues [21]. This makes it an ideal candidate for the potential for stem cells in medical applications [26]. Although hUC-MSCs have good bone induction, they are easy to be absorbed and degraded in vivo. Collagen is one of the most widely used bone-filling biomaterial in present bone tissue engineering [27]. However, studies have shown that the function of collagen-based biomaterials in bone repair alone is limited [28]. Collagen scaffold material can be used as an ideal scaffold material to enable HUC-MSCs to better act on bone defect sites [23]. The combination of collagen scaffolds can slow down the degradation rate of hUC-MSCs, thus prolonging the bone repair time.

Bone collagen particles used in this study are heterogeneous bone made from bovine cancellous bone after degreasing and decellularization. Bone matrix particles are mainly composed of hydroxyapatite and collagen. The material has high strength, strong bone conductivity and good biological safety. The bone matrix retains a natural three-dimensional network that facilitates cell implantation and growth. After decellularization, the allogeneic bone can effectively reduce its immunogenicity [29]. Heterogeneous bone matrix is more widely derived than allograft bone, and the degradation and absorption time is shorter, all of which meet the requirements of ideal carrier. Newly formed bone tissue was identified in the defect areas of MSCs groups by micro-CT and various staining methods. As expected, the MSCs group was more effective than the material group. To the best of our knowledge, this study is the first designed to evaluate the effects of bone collagen particles combined with UC-MSCs on incisor bone regeneration for 3 months and 6 months.

Although HUC-MSCs have been successfully used in the treatment of various bone lesions in vivo [30-32], the environment of the incisor is quite different from other sites in terms of the force, stress and movement of the alveolar bone. Therefore, the therapeutic strategy for alveolar bone defects needs to be re-evaluated.

The purpose of this study was to evaluate the effect of bone collagen particles combined with hUC-MSCs on the repair of alveolar bone defects. Serological detection is a comprehensive detection of body function, which is very important in the assessment of the biosafety of bone collagen particles and hUC-MSCs in vivo. Routine blood tests are often used to detect inflammation and early detection of disease. Liver function test can reflect the liver injury. Kidney function testing is used to assess kidney function, which in turn can reflect the health of the kidney. C-reactive protein is highly sensitive to infectious inflammation [33]. BGP is produced and released directly from osteoblasts. BGP was positively correlated with bone formation. If the biological safety of the material is good, the blood indicators will not be significantly different from that of the normal group. The results of the blood test showed that the bone collagen particles and hUC-MSCs had good biological safety, and that the hUC-MSCs could reduce the inflammatory response. We speculate that bone collagen particles and hUC-MSCs do not significantly change the physiological environment of the body in the absorption process like metal alloy materials [35-37]. In addition, the main components of bone collagen particles are hydroxyapatite and collagen type I, which can effectively reduce its immunogenicity. The immunogenicity of hUC-MSCs is also relatively low [22]. Gross observation of the skull model and Micro CT scans results showed that the effect of bone collagen particles combined with hUC-MSCs on bone regeneration and repair was stronger than that of bone collagen particles alone. Tissue staining results also showed that the bone collagen particles combined with hUC-MSCs had significantly increased trabecular bone formation rate. Studies have shown that the formation of new bone depends on bone trabecular density and connection rate, etc [38]. The number of osteoblasts and chondrocytes was also significantly increased. The expression levels of collagen 1 was significantly higher than those in the material group. The results of cell proliferation and apoptosis suggested that the combination of bone collagen particles with hUC-MSCs could further promote cell proliferation and apoptosis, thus promoting bone regeneration.

Bone induction refers to the induction into connective tissue adjacent to bone graft by certain factors of bone materials. By affecting undifferentiated bone progenitor cells and promoting their differentiation and proliferation, they eventually become osteoblasts and promote the formation of new bone [39]. The alveolar cleft model established in this study is a hole formed by pulling out the incisor [8]. After removing the incisors, the damage to the inner wall of the bone around the incisors was not obvious except for the root of the incisors. Therefore, the osteogenic induction ability of different positions was not uniform after the addition of bone collagen particles. Although there was still a certain gap between the newly generated bone from bone collagen particles combined with hUC-MSCs and the normal incisor, it was enough to prove that hUC-MSCs could be used as bone generation inducer combined with bone materials for bone regeneration and repair. In the near future, it may be used for tissue engineering bone regeneration with potential clinical application value.

## Conclusions

With the development of tissue engineering technology, it is difficult to achieve the goal of bone repair simply by using scaffold materials. The combination of hUC-MSCs with biomaterials is a promising strategy in the field of regenerative medicine and bone repair. In this study, it was found that the effect of bone collagen granule combined with hUC-MSCs on bone repair and regeneration was much better than that of bone collagen particles alone. The method of hUC-MSCs combined with bone collagen particle material to fill a bone defect site is simple, rapid and suitable for the treatment of alveolar cleft bone defects. It is considered as a promising method for reconstruction of incisor bone defects.

## Materials And Methods

### Isolation & culture of HUC-MSCs

HUC-MSCs were isolated from Wharton's jelly. In this study, tissue blocks adherent culture was used to isolate hUC-MSCs. The blood vessels in the umbilical cord were first removed and the tissue cut into about 1 cubic millimeter pieces. The tissue blocks were inoculated in a 10cm petri dish and then Stand it upside down for 4 hours in an incubator at 37°C with 5%CO<sub>2</sub> for 4 hours. After the tissue blocks were fixed at the bottom of the plate, α-MEM complete medium was added for primary culture. After about 2 weeks, the cells crawled out in a radial manner. At this time, the cell suspension was collected and centrifuged in a 15 ml centrifuge tube at 800 r/min for 5 min. The supernatant was discarded and gently blown into a single-cell suspension for subculture. HUC-MSCs within five generations were collected to incubate bone collagen particles.

### Preparation of implant materials

Bone collagen particles are made of bovine cancellous bone by special decellularization and degreasing process. Its main components are hydroxyapatite and collagen I, which can effectively reduce its immunogenicity. It also preserves the natural structure of the bone, which is good for the growth of cells



and blood vessels. The bone collagen particles were provided by zhenghai biotechnology Co. LTD (Yantai, China). Cells within 5 generations were selected to be inoculated with bone collagen particles and cultured in carbon dioxide incubator for 0.5 h. The concentration of hUC-MSCs should reach  $10^7$  cells/ml.

### **Surgical procedure & treatment (Figure 1)**

In this study, we used 24 female JWRs (bodyweight:  $2000\pm 300$  g). These JWRs were purchased from huafukang biotechnology Co. LTD (Beijing, China). All these animals were kept in the animal room of National Research Institute for Family Planning, with free access to water and food. Temperature controls in the 23 to 25 °C. Humidity of 50% to 60%. Noise controls under 60dB. The light cycle is 12h for day and night. Keep the room clean, dry and ventilated. The study was approved by the local research and ethics committee.

Twenty-four JWRs were randomly divided into four groups (n=6 in each group): normal group, control group, material group and MSCs group. Rabbits were anesthetized by intravenous injections of serazine hydrochloride (concentration: 1-2mg/kg). The model of alveolar clefts was established by removing the incisors on the left side of the upper jaw (Figure 1f-h). The normal group was fed normally without surgery. In the control group, collagen membrane was directly covered and skin was sutured after incisors was removed. In the material group, after the incisions were removed, the holes were filled with bone collagen particles, and then the collagen membrane was covered and the skin was sutured. In the MSCs group, after the incisions were removed, the holes were filled with bone collagen particles incubated by hUC-MSCs, and then the collagen membrane was covered and the skin was sutured. The rabbits were treated with antibiotics for 1 week to prevent infection. Blood was collected from each group at 3 and 6 months after surgery. All rabbits were euthanized and the upper jaw was examined and obtained for further evaluation.

### **Blood analysis**

At 3 months after the surgery, 3 rabbits were randomly selected from each group. Blood routine, liver function, kidney function and BGP of rabbits were detected by collecting 3.5ml of venous blood from the ears. 1ml of whole blood was used for routine blood testing. The serum was isolated from the remaining 2.5ml of whole blood, and then the serum was used for blood biochemistry testing. Routine blood tests were performed using LH 750 automated hematology analyzer (Beckman Coulter, U.S.A). The blood biochemistry test used DXC 800 automated biochemical analyzer (Beckman Coulter, U.S.A). At 6 months after the surgery, the indexes of the remaining 3 rabbits were detected.

### **Micro CT analysis**

3 months after the surgery, one rabbit was randomly selected from each group to make a skull model. The procedure was repeated 6 months after surgery. The skull was photographed to record its appearance. Bone regeneration in the skull was evaluated by micro CT. Bone regeneration in the alveolar cleft was evaluated using a micro CT system (SIEMENS Inveon Research Workplace 4.2, Beijing). The

three-dimensional repair of the injuries to each group was observed, and the trabecular bone and bone density values were recorded.

## **Histology staining**

Rabbits were euthanized and histologically evaluated at 3 or 6 months postoperatively. The specimens were immersed in 4% paraformaldehyde for 24h and then decalcified in 10% EDTA. After decalcification, the tissue was first embedded in paraffin, and then paraffin sections with a thickness of 4um were prepared by the microtome.

The morphology of the cells was revealed by hematoxylin eosin (HE) staining. The nuclei are stained blue-violet by hematoxylin and the other tissue can be stained red by eosin. The secret products of chondrocytes are metachromatic and can eventually differentiate into osteoblasts. Periodic Acid-Schiff stains (PAS) staining can dye chondrocytes dark purple or crimson. Collagen type 1 is found mainly in bone and tendon fibers and can be dyed bright orange by Sirius red. We also used Image J software to calculate the relative percentage of the positive staining area in each section. Osteoblasts are one of the markers for bone formation. Black cobalt sulfide deposits can be formed by alkaline phosphatase (ALP) colorimetry for the location of osteoblasts.

Bone morphogenetic protein 2 (MSCS2) is one of the markers for bone formation. Primary anti-MSCS2 (ab6285, 1:1000 dilution; Abcam Ltd) and HRP coupled secondary antibody were used to detect the positioning in slices. Ki67 can be used to locate proliferating cells. Primary anti-Ki67 (ab15580, 1:1000 dilution; Abcam Ltd) was used to detect cell proliferation by immunofluorescence. TUNEL can be used to locate apoptotic cells. Three regions were randomly selected and the percentage of Ki67 and TUNEL positive cells was quantified using Image J software.

## **Statistical analysis**

All values are expressed as the mean  $\pm$  SD.  $P < 0.05$  indicates statistical significance. Data were analyzed statistically by factorial analysis of variance and the Student's t-test with GraphPad Prism software (GraphPad Prism 6).

## **Abbreviations**

human umbilical cord mesenchymal stem cells (HUC-MSCs)

JWRs (Japanese white rabbits)

micro CT (microfocus computerized tomography)

hematoxylin eosin (HE)

alkaline phosphatase  $\square$ ALP  $\square$

PeriodicAcid-Schiff stain (PAS)

immunohistochemical(IHC)

## **Declarations**

### **Ethics approval and consent to participate**

The study was approved by the ethics committee of the National Research Institute for Family Planning.

### **Consent for publication**

Not applicable

### **Availability of data and materials**

All data generated or analysed during this study are included in this published article.

### **Competing interests**

The authors declare that they have no competing interests.

### **Funding**

This work was funded by grants from the National Key Research and Development Program of China (2016YFC1000803).

### **Authors' contributions**

XCS, XM and HFX designed the study. XCS, HW and JHL were responsible for the vivo surgery and performing the procedure. XCS was responsible for in vitro experiments. XCS, HW were responsible for HUC-MSCs culture. XCS, HW and HFX prepared the manuscript. XCS, HW, DZ and HFX were responsible for revising the manuscript critically for important intellectual content. All authors read and approved the final manuscript.

### **Acknowledgements**

The authors are very grateful to the National Key Research and Development Program of China. We are also very grateful to the animal experiment center of the National Research Institute for Family Planning for its meticulous care of animals.

### **Authors' details**

a Reproductive and Genetic Center of National Research Institute for Family Planning, Beijing, 10081, China

## References

- [1]Harvold, Egil. Cleft Palate, An Experiment[J]. Acta Odontologica Scandinavica, 1950, 9(1):84-87.
- [2]Chierici G , Harvold E P , Dawson W J . Primate Experiments on Facial Asymmetry[J]. Journal of Dental Research, 1970, 49(4):847-851.
- [3]Longaker M T , Stern M , Lorenz H P , et al. A Model for Fetal Cleft Lip Repair in Lambs[J]. Plastic and Reconstructive Surgery, 1992, 90(5):750-756.
- [4]Weinberg M A , Bral M . Laboratory animal models in periodontology[J]. Journal Of Clinical Periodontology, 1999, 26(6):335-340.
- [5]Liao L S , Tan Z , Zheng Q , et al. Animal experimental study on repairing alveolar clefts by using rectilinear distraction osteogenesis[J]. Journal of Plastic Reconstructive & Aesthetic Surgery, 2009, 62(12):1573-1579.
- [6]Dalia E B , Smith S J , Germane N , et al. New Technique for Creating Permanent Experimental Alveolar Clefts in a Rabbit Model[J]. The Cleft Palate-Craniofacial Journal, 1993, 30(6):542-547.
- [7]Bardach J , Kelly K M . Role of Animal Models in Experimental Studies of Craniofacial Growth Following Cleft Lip and Palate Repair[J]. The Cleft palate journal, 1988, 25(2):103-113.
- [8]Xue-Cheng Sun,Ze-Biao Zhang et al. Comparison of three surgical models of bone tissue defects in cleft palate in rabbits[J]. International Journal of Pediatric Otorhinolaryngology.2019;124:164-172.
- [9]Binger T , Katsaros C , Martin Rücker, et al. Segment Distraction to Reduce a Wide Alveolar Cleft Before Alveolar Bone Grafting[J]. The Cleft Palate-Craniofacial Journal, 2003, 40(6):561-565.
- [10]Boyne P J . Secondary bone grafting of residual alveolar and palatal clefts[ J] .J Oral Surg, 1972, 30( 2) :87-92.
- [11]Cohen M , Figueroa A A , Haviv Y , et al. Iliac Versus Cranial Bone for Secondary Grafting of Residual Alveolar Clefts[J]. Plastic and Reconstructive Surgery, 1991, 87(3):423-427.
- [12]Tai C C E , Sutherland I S , Mcfadden L . Prospective analysis of secondary alveolar bone grafting using computed tomography [J]. Journal of Oral & Maxillofacial Surgery Official Journal of the American Association of Oral & Maxillofacial Surgeons, 2000, 58(11):1241-1249.
- [13]Nique T , Fonseca R J , Upton L G , et al. Particulate allogeneic bone grafts into maxillary alveolar clefts in humans: A preliminary report[J]. Journal of Oral and Maxillofacial Surgery, 1987, 45(5):386-392.

- [14]El Deeb M , Tompach P C , Morstad A T , et al. Long-term follow-up of the use of nonporous hydroxyapatite for augmentation of the alveolar ridge[J]. *Journal of oral and maxillofacial surgery: official journal of the American Association of Oral and Maxillofacial Surgeons*,1991,49(3):257-261.
- [15]Chan B P , Hui T Y , Wong M Y , et al. Mesenchymal Stem Cell–Encapsulated Collagen Microspheres for Bone Tissue Engineering[J]. *TISSUE ENGINEERING PART C-METHODS*, 2010, 16(2):225-235.
- [16]Johnson K D, Frierson K E, Keller T S , et al. Porous ceramics as bone graft substitutes in long bone defects: A biomechanical, histological, and radiographic analysis[J]. *Journal of Orthopaedic Research*, 1996, 14(3):351-369.
- [17]Shuai C, Zhou J, Wu P, et al. Enhanced Stability of Calcium Sulfate Scaffolds with 45S5Bioglass for Bone Repair [J]. *Materials*,2015, 8(11):7498-7510.
- [18] Smith BT, Santoro M, Grosfeld EC, et al. Incorporation of fast dissolving glucose porogens into an injectable calcium phosphate cement for bone tissue engineering [J]. *Acta Biomaterialia*, 2016, 50, Mar 1, 68-77.
- [19]Rahaman MN, Day DE, Bal BS, et al. Bioactive glass in tissue engineering. *Acta Biomater*, 2011, 7(6): 2355-2373.
- [20]Hibi H , Yamada Y , Ueda M , et al. Alveolar cleft osteoplasty using tissue-engineered osteogenic material[J]. *International Journal of Oral & Maxillofacial Surgery*, 2006, 35(6):551-555.
- [21]Liu S , Hou K D , Yuan M , et al. Characteristics of mesenchymal stem cells derived from Wharton's jelly of human umbilical cord and for fabrication of non-scaffold tissue-engineered cartilage[J]. *Journal of Bioscience & Bioengineering*, 2014, 117(2):229-235.
- [22]Jin YZ, Lee JH. Mesenchymal stem cell therapy for bone regeneration. *Clin. Orthop. Surg.* 10(3), 271–278 (2018).
- [23]Tassi S A , Sergio N Z , Misawa M Y O , et al. Efficacy of stem cells on periodontal regeneration: Systematic review of pre-clinical studies[J]. *Journal of Periodontal Research*, 2017, 52(5): 793-812.
- [24] Li X, Tan J, Xiao Z et al. Transplantation of hUC-MSCs seeded collagen scaffolds reduces scar formation and promotes functional recovery in canines with chronic spinal cord injury. *Sci. Rep.* 7, 43559 (2017).
- [25]Campisi P, Handy RC, et al. Expressing of bone morphogenetic protein during mandibular distraction osteogenesis[J]. *Plast Reconstr Surg*,2003;111:201-208.
- [26] Wang Limin, Tran I, Seshareddy K, et al. A comparison of human bone marrow-derived mesenchymal stem cells and human umbilical cord-derived mesenchymal stromal cells for cartilage tissue engineering [J]. *Tissue Eng A*, 2009,15(8):2259-2266.

- [27] Liu LS, Thompson AY, Heidarman MA, Poser JW, Spiro RC. An osteoconductive collagen/ hyaluronate matrix for bone regeneration. *Biomaterials* 1999;20(12):1097–108.
- [28] Hollinger JO, Schmitt JM, Buck DC, Shannon R, Joh SP, Zegzula HD, et al. Recombinant human bone morphogenetic protein-2 and collagen for bone regeneration. *J Biomed Mater Res* 1998;43(4):356–64.
- [29] Böer U, Lohrenz A, Klingenberg M, et al. The effect of detergent-based decellularization procedures on cellular proteins and immunogenicity in equine carotid artery grafts. *Biomaterials*, 2011, 32(36): 9730-9737.
- [30] Song K, Yang Y, Xu L et al. Fabrication and detection of tissue engineered bone aggregates based on encapsulated human ADSCs within hybrid calcium alginate/bone powder gel-beads in a spinner flask. *Mater. Sci. Eng. C Mater. Biol. Appl.* 62, 787–794 (2016).
- [31] Wang N, Xiao Z, Zhao Y et al. Collagen scaffold combined with human umbilical cord-derived mesenchymal stem cells promote functional recovery after scar resection in rats with chronic spinal cord injury. *J. Tissue. Eng. Regen. Med.* 12(2), e1154–e1163 (2018).
- [32] Shin M, Yoshimoto H, Vacanti JP. In vivo bone tissue engineering using mesenchymal stem cells on a novel electrospun nanofibrous scaffold. *Tissue Eng* 2004;10(1–2):33–41.
- [33] Mooiweer E, Luijck B, Bonten MJ, et al. C-reactive protein levels but not CRP dynamics predict mortality in patients with pneumococcal pneumonia. *J Infect*, 2011, 62 (4):313-316
- [34] Cosman F, Nieves J, Zion M, et al. Daily and cyclic parathyroid hormone in women receiving alendronate. *NEngl J Med* 2005;353(6):566–575.
- [35] Han P, Cheng P, Zhang S, et al. In vitro and in vivo studies on the degradation of high-purity Mg (99.99wt.% ) screw with femoral intracondylar fractured rabbit model[J]. *Biomaterials*, 2015, 64: 57-69
- [36] Sotoudehbagha P, Sheibani S, Khakbiz M, et al. Novel antibacterial biodegradable Fe-Mn-Ag alloys produced by mechanical alloying[J]. *Mater Sci Eng C Mater Biol Appl*, 2018, 88: 88-94
- [37] Mostaed E, Sikora-Jasinska M, Drelich J W, et al. Zinc-based alloys for degradable vascular stent applications [J]. *Acta Biomater*, 2018, 71: 1-23
- [38] Cramer JA, Gold DT, Silverman SL, et al. A systematic review of persistence and compliance with bisphosphonates for osteoporosis. *Osteoporos Int.* 2007;18(8):1023-1031.
- [39] zur Nieden NI, Kempka G, Ahr HJ. In vitro differentiation of embryonic stem cells into mineralized osteoblasts. *Differentiation* 2003;71:18-27.

## Tables

**Table 1 Blood routine test results at 3 months postoperatively**

Detection index	Unit	Normal group	Control group	Material group	MSCs group
RBC	10 <sup>12</sup> /L	5.727±0.460	5.757±0.802	5.660±0.067	4.803±0.759
HCT	%	36.467±2.120	37.867±2.839	37.300±1.631	31.167±4.619
RDW-CV	10 <sup>9</sup> /L	13.033±0.873	14.400±0.589	13.333±0.262	15.267±2.864
RDW-SD	%	29.400±2.192	33.767±3.420	30.867±1.793	35.367±7.014
MCV	fL	63.800±1.344	66.367±4.739	65.133±2.593	64.900±1.283
HBG	g/L	117.667±6.182	123.000±13.491	121.000±2.944	103.333±16.680
MCH	pg	20.600±0.980	21.433±0.910	21.100±0.455	21.433±0.450
MCHC	g/L	323.000±10.033	323.667±10.965	324.667±8.179	330.667±13.123
WBC	10 <sup>9</sup> /L	13.170±2.788	8.680±2.961	10.037±1.848	8.603±1.062
LYM#	10 <sup>9</sup> /L	4.685±0.672##	2.243±0.452**	2.318±0.183**	3.195±0.428*
LYM%	%	36.080±2.401	28.633±9.420	23.670±3.746	37.130±2.007
NEUT#	10 <sup>9</sup> /L	7.547±2.054	5.652±2.275	6.606±1.369	4.589±0.761
NEUT%	%	56.617±3.356	63.050±6.846	65.517±2.569	53.220±4.038
MONO#	10 <sup>9</sup> /L	0.664±0.132	0.579±0.329	0.780±0.267	0.492±0.141
MONO %	%	5.120±0.889	5.923±2.294	7.573±1.156	5.740±1.511
EO#	10 <sup>9</sup> /L	0.229±0.022	0.153±0.070	0.320±0.113	0.235±0.047
EO %	%	1.800±0.318	1.710±0.513	3.090±0.565	2.760±0.556
BASO	10 <sup>9</sup> /L	0.045±0.017	0.052±0.033	0.016±0.003	0.092±0.043
BASO %	%	0.383±0.210	0.683±0.363	0.150±0.037	1.150±0.689
PLT	10 <sup>9</sup> /L	153.333±35.188	171.667±22.867	141.000±24.536	127.667±8.498
PDW	%	15.700±0.294	15.967±0.403	15.967±0.478	15.533±0.047
MPV	fL	7.167±0.411	7.133±0.249	7.300±0.653	6.767±0.450
PLCR	%	14.267±4.606	14.833±3.167	14.300±3.511	10.567±1.761
PCT	%	0.041±0.021	0.028±0.011	0.038±0.030	0.013±0.005
CRP	mg/l	6.400±1.425	12.433±4.488	6.870±3.556	3.143±2.191#

Mean SD values were calculated for each group. \* represents the statistical difference between each group and the normal group. # represents the statistical difference between each group and the control group. \*, # P<0.05; \*\*, ## P<0.01. RBC:red blood cell; HCT: hematocrit; RDW-CV: red blood cell volume distribution width; RDW-SD: red blood cell distribution width ; MCV: mean corpuscular volume ; HBG: hemoglobin; MCH: mean corpuscular hemoglobin; MCHC: mean corpuscular hemoglobin concentration ; WBC: white blood cell; LYM: lymphocyte; NEUT: neutrophile granulocyte; MONO: monocyte; EO: eosinophil; BASO: basophil; PLT: platelet; PDW: platelet distribution width; MPV: mean

platelet volume; PLCR: platelet-large cell ratio; PCT: platelet volume; CRP: C reactive protein.

**Table 2 Liver function test results in blood at 3 months postoperatively**

Detection index	Unit	Normal group	Control group	Material group	MSCs group
ALT	IU/L	44.533±5.424	82.167±23.572	62.333±7.903	41.400±11.051#
AST	IU/L	30.567±6.215	76.000±48.880	44.833±29.613	16.167±2.595
ALP	IU/L	47.000±17.705	59.767±10.700	67.400±13.983	23.867±5.188
TP	g/l	52.533±0.694	58.000±3.827	59.133±2.845	48.900±7.920
ALB	g/l	33.500±0.424	38.633±3.307	36.667±1.066	27.900±7.896
GLB	g/l	19.000±1.042	19.400±2.825	22.467±3.561	21.000±2.140
A/G		1.767±0.119	2.040±0.381	1.680±0.299	1.347±0.411
TBIL	Umol/L	9.247±1.036	8.080±1.408	8.917±2.806	6.953±0.345
DBIL	Umol/L	5.093±0.718	3.870±0.388	4.817±0.749	2.977±0.310*
IBIL	Umol/L	4.153±1.311	4.210±1.632	4.100±2.088	3.977±0.553

Mean SD values were calculated for each group. \* represents the statistical difference between each group and the normal group. # represents the statistical difference between each group and the control group. \*, # P<0.05. ALT: alanine aminotransferase; AST: aspartate aminotransferase; ALP: alkaline phosphatase; TP: total protein; ALB: albumin; GLB: globulin; TBIL: total bilirubin; DBIL: bilirubin direct; IBIL: indirect bilirubin.

**Table 3 Renal function results test in blood at 3 months postoperatively**

Detection index	Unit	Normal group	Control group	Material group	MSCs group
BUN	mmol/L	7.647±1.540	9.233±3.682	7.247±2.116	11.227±4.190
CR	mmol/L	69.707±7.026	103.413±27.201	94.840±15.769	107.587±27.686
UA	mmol/L	31.467±2.155	30.733±1.126	29.600±0.141	29.700±0.000

Mean SD values were calculated for each group. BUN: blood urea nitrogen CR: creatinine UA: uric acid.

**Table 4 Blood routine test results at 6 months postoperatively**



Detection index	Unit	Normal group	Control group	Material group	MSCs group
RBC	$10^{12}/L$	5.467±0.364	4.927±0.190	4.250±0.964	5.433±0.233
HCT	%	36.067±1.636	36.400±4.369	26.933±5.949	33.867±2.014
RDW-CV	$10^9/L$	13.200±0.356	12.567±0.865	12.567±1.096	12.833±0.759
RDW-SD	%	30.967±2.253	31.433±2.782	28.600±2.128	29.300±1.203
MCV	fL	66.133±3.642	70.400±2.264	63.500±0.920	64.000±2.551
HBG	g/L	123.000±2.944	122.000±10.801	92.667±18.571	115.333±6.944
MCH	pg	22.600±0.990	23.667±0.732	21.967±0.713	21.800±0.920
MCHC	g/L	342.000±8.832	336.000±10.614	345.667±7.587	340.667±1.886
WBC	$10^9/L$	10.727±0.281	8.347±0.241	9.167±2.172	10.777±1.829
LYM#	$10^9/L$	3.700±0.009	2.299±0.544	2.908±0.603	3.947±0.737#
LYM%	%	34.517±0.926	27.457±5.857	32.310±4.066	36.503±0.922
NEUT#	$10^9/L$	6.165±0.287	5.265±0.285	5.518±1.541	5.913±0.946
NEUT%	%	57.443±1.217	63.157±4.320	59.440±4.470	55.020±1.007
MONO#	$10^9/L$	0.566±0.024	0.580±0.134	0.565±0.106	0.557±0.101
MONO %	%	5.280±0.204	6.977±1.724	6.390±1.289	5.167±0.118
EO#	$10^9/L$	0.264±0.088	0.169±0.012	0.158±0.110	0.330±0.045
EO %	%	2.470±0.853	2.000±0.163	1.643±0.845	3.090±0.127
BASO	$10^9/L$	0.032±0.013	0.017±0.004	0.019±0.002	0.023±0.009
BASO %	%	0.360±0.060	0.175±0.025	0.217±0.029	0.220±0.057
PLT	$10^9/L$	137.333±13.695	148.667±20.997	156.333±39.878	126.333±8.380
PDW	%	15.800±0.163	15.833±0.403	15.733±0.205	16.233±0.125
MPV	fL	7.167±0.189	6.867±0.205	6.800±0.294	6.900±0.141
PLCR	%	13.400±1.349	11.367±1.247	11.467±3.055	13.500±1.980
PCT	%	0.027±0.012	0.030±0.014	0.040±0.029	0.017±0.005
CRP	mg/l	4.373±1.426	3.990±0.670	14.663±12.212	3.957±0.651

Mean SD values were calculated for each group. RBC:red blood cell; HCT: hematocrit; RDW-CV: red blood cell volume distribution width; RDW-SD: red blood cell distribution width ; MCV: mean corpuscular volume ; HBG: hemoglobin; MCH: mean corpuscular hemoglobin; MCHC: mean corpuscular hemoglobin concentration; WBC: white blood cell; LYM: lymphocyte; NEUT: neutrophile granulocyte; MONO: monocyte; EO: eosinophil; BASO: basophil; PLT: platelet; PDW: platelet distribution width; MPV: mean platelet volume; PLCR: platelet-large cell ratio; PCT: platelet volume; CRP: C reactive protein.

**Table 5 Liver function test results in blood at 6 months postoperatively**

Detection index	Unit	Normal group	Control group	Material group	MSCs group
ALT	IU/L	72.733±17.093	122.400±102.499	50.700±58.432	50.800±10.968
AST	IU/L	23.567±1.126	32.167±14.290	15.400±11.052	23.400±0.294
ALP	IU/L	60.567±10.076	59.933±25.986	39.800±20.467	58.567±4.615
TP	g/l	62.000±0.648	62.433±3.058	58.633±21.150	60.167±2.829
ALB	g/l	40.600±1.283	38.400±5.233	35.367±12.761	38.800±2.765
GLB	g/l	21.367±1.698	24.033±2.323	23.300±7.763	21.333±3.583
A/G		1.917±0.222	1.633±0.349	1.540±0.554	1.893±0.438
TBIL	Umol/L	4.807±0.813	6.710±1.714	6.720±0.070	3.570±0.536
DBIL	Umol/L	2.123±0.229	4.057±1.500	3.557±1.415	2.333±0.352
IBIL	Umol/L	2.683±0.877	2.653±0.476	2.160±0.854	1.237±0.189

Mean SD values were calculated for each group. ALT=alanine aminotransferase; AST: aspartate aminotransferase; ALP: alkaline phosphatase; TP: total protein; ALB: albumin; GLB: globulin; TBIL: total bilirubin; DBIL: bilirubin direct; IBIL: indirect bilirubin.

**Table 6 Renal function results test in blood at 6 months postoperatively**

Detection index	Unit	Normal group	Control group	Material group	MSCs group
BUN	mmol/L	8.763±0.403	8.570±1.241	8.263±2.780	7.987±1.025
CR	mmol/L	99.877±7.261	100.123±4.054	88.000±32.339	89.457±8.307
UA	mmol/L	33.633±3.175	30.067±1.819	30.000±10.322	29.133±0.694

Mean SD values were calculated for each group. BUN: blood urea nitrogen CR: creatinine UA: uric acid.

## Figures



**Figure 1**

surgical process: a collagen granules were incubated by hUC-MSCs. b fix the anaesthetized rabbits. c open the oral cavity after anesthesia. d-e incise the skin f-h remove the left incisor. i-j add collagen particles. k-l suture the skin .

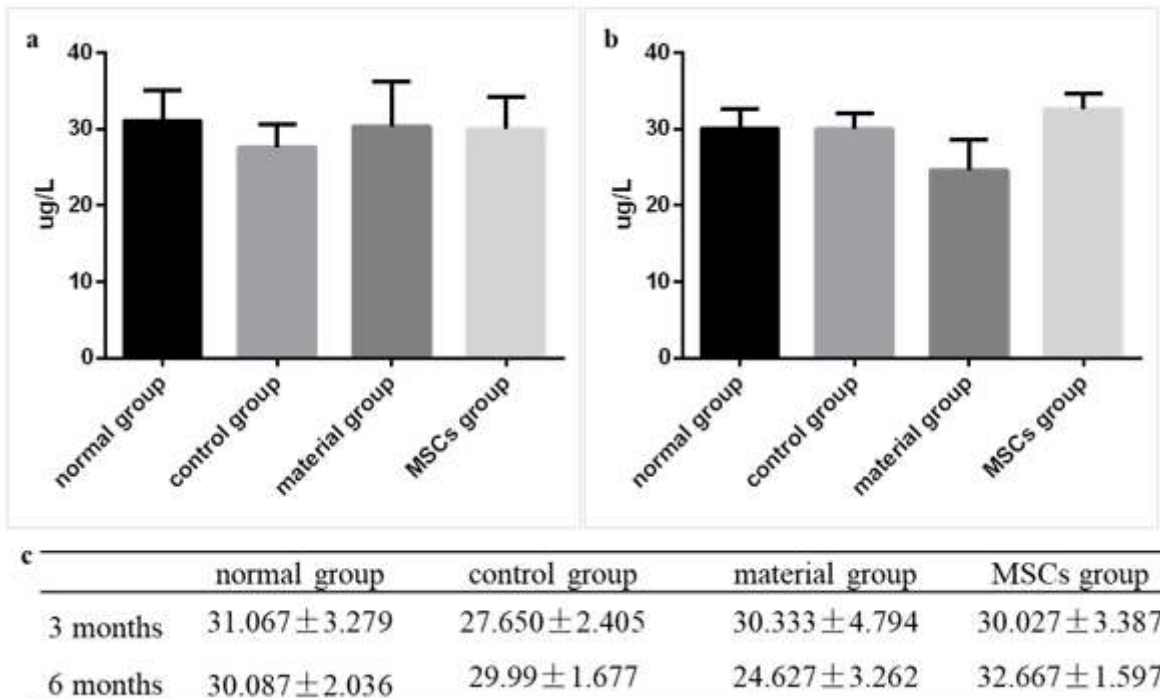


**Figure 2**

a: the content of serum BGP in each group at 3 months; b: the content of serum BGP in each group at 6 months; c: Statistical analysis of BGP results at 3 and 6 months postoperatively (mean±SD).

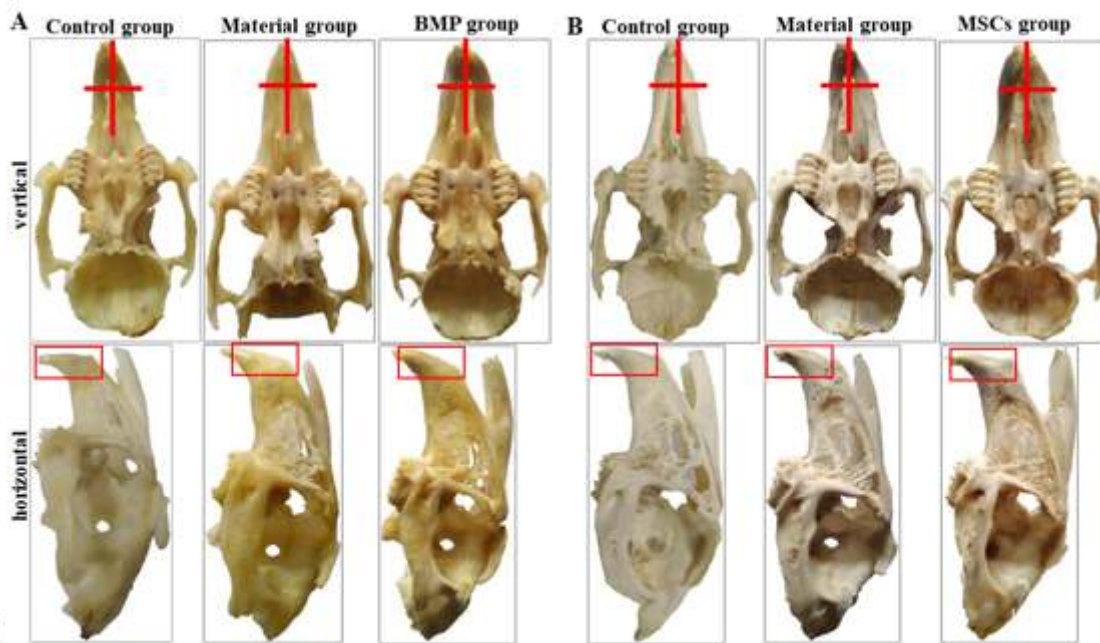


**Figure 3**

The general appearance of the skull and the red box is the surgical area. A sampling group 3 months after surgery; B sampling group 6 months after surgery. The red box and red plus sign assist in displaying the recovery of the transplanted area.

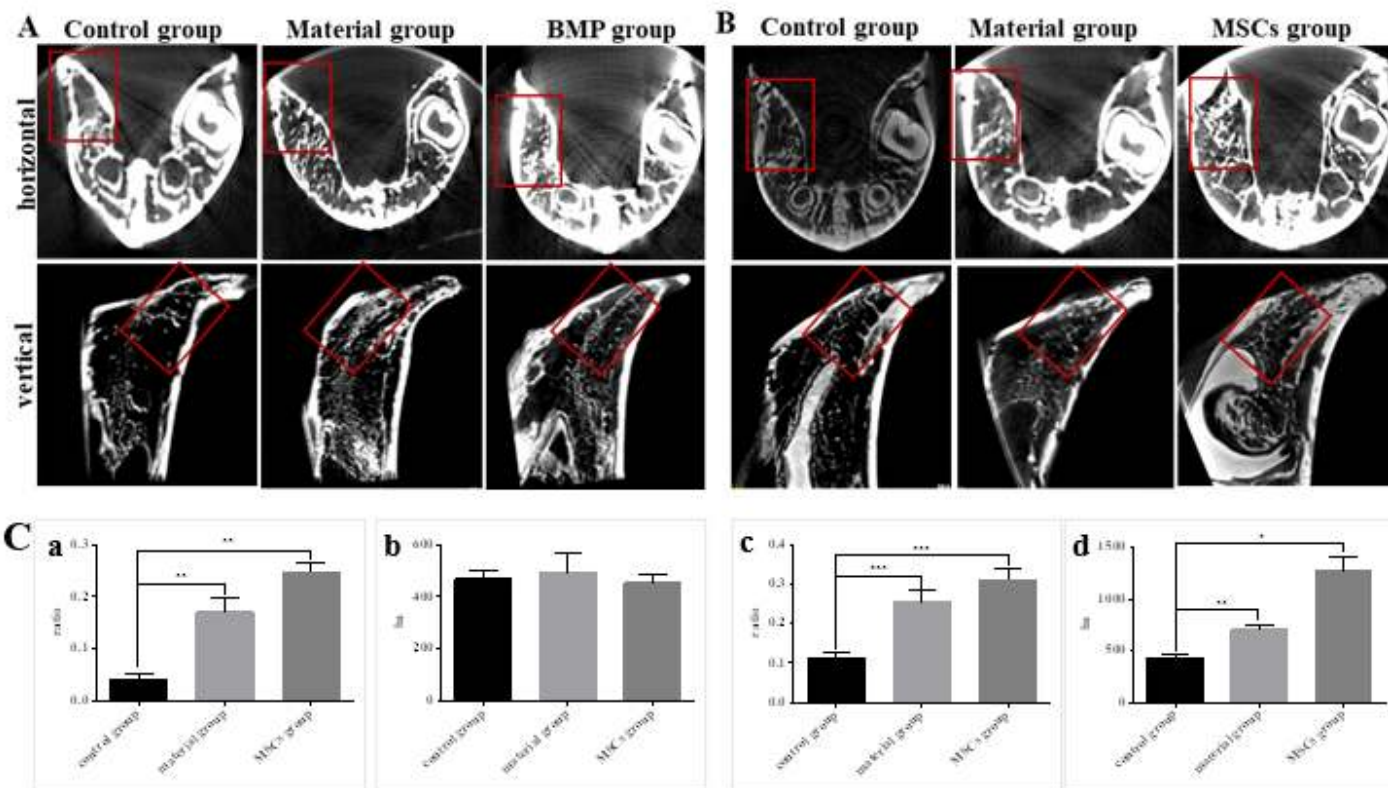


**Figure 4**

Micro CT results. A CT images from different angles at 3 months; B CT images from different angles at 6 months; C-a: the percentage of bone trabeculae at 3 months after surgery; C-b: the percentage of bone mineral density percentage at 3 months after surgery; C-c: the percentage of bone trabeculae at 6 months after surgery; C-d: the percentage of bone mineral density at 6 months after surgery. All groups were compared with the control group, and the difference was expressed as \*.The red box represents the surgical area.

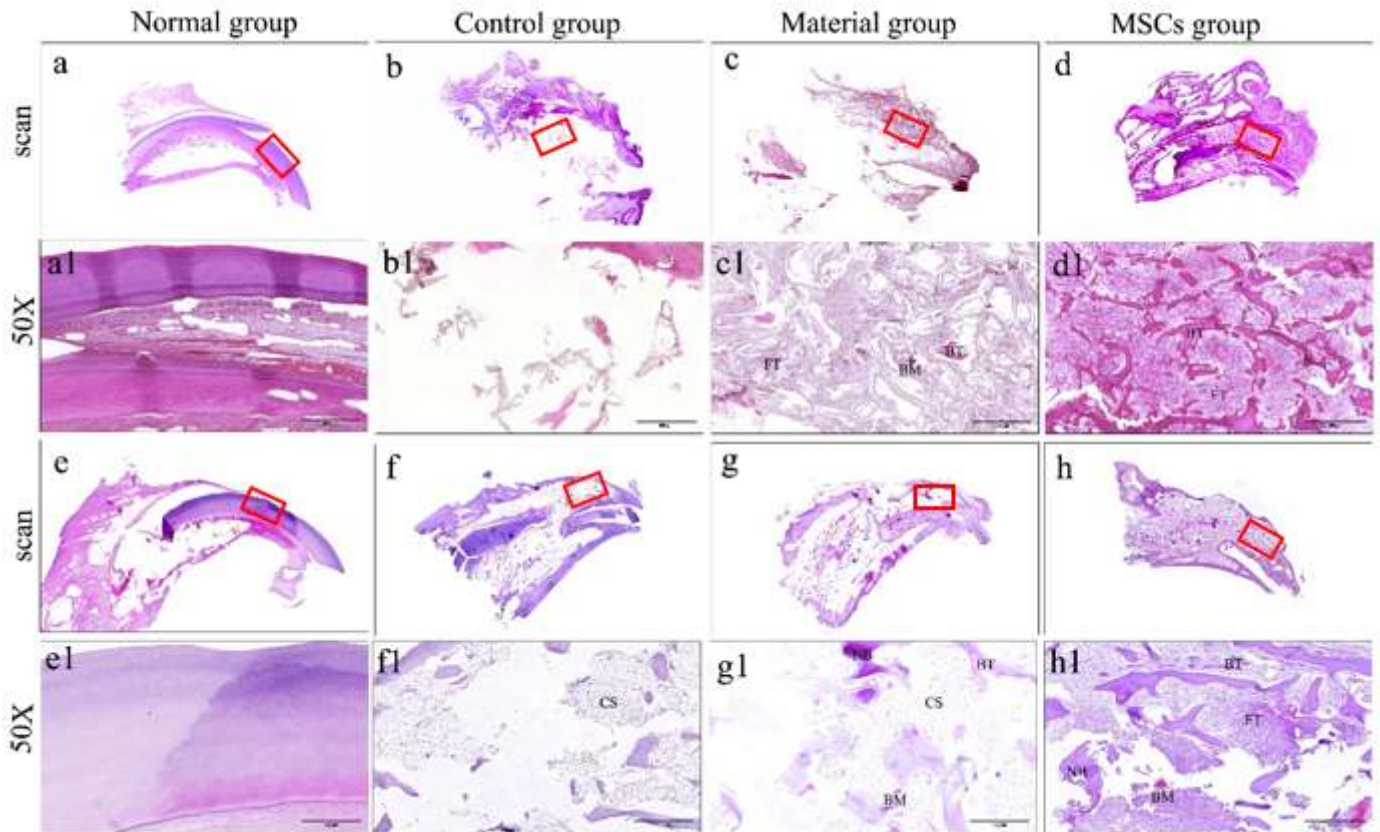


**Figure 5**

HE staining results. a-d & a1-d1 Sampling group 3 months after surgery; e-h & e1-h1 Sampling group 6 months after surgery. a,e & a1,e1 Normal group b,f & b1,f1 Control group c, g & c1, g1 Material group d, h & d1, h1 MSCs group. a-h The scan results of HE staining. a1-h1 The result of HE staining after 50 times magnification. BM: bone marrow; FT: fibrous tissue; BT: bone trabecula; NB: new bone; CS: cavitation structure.

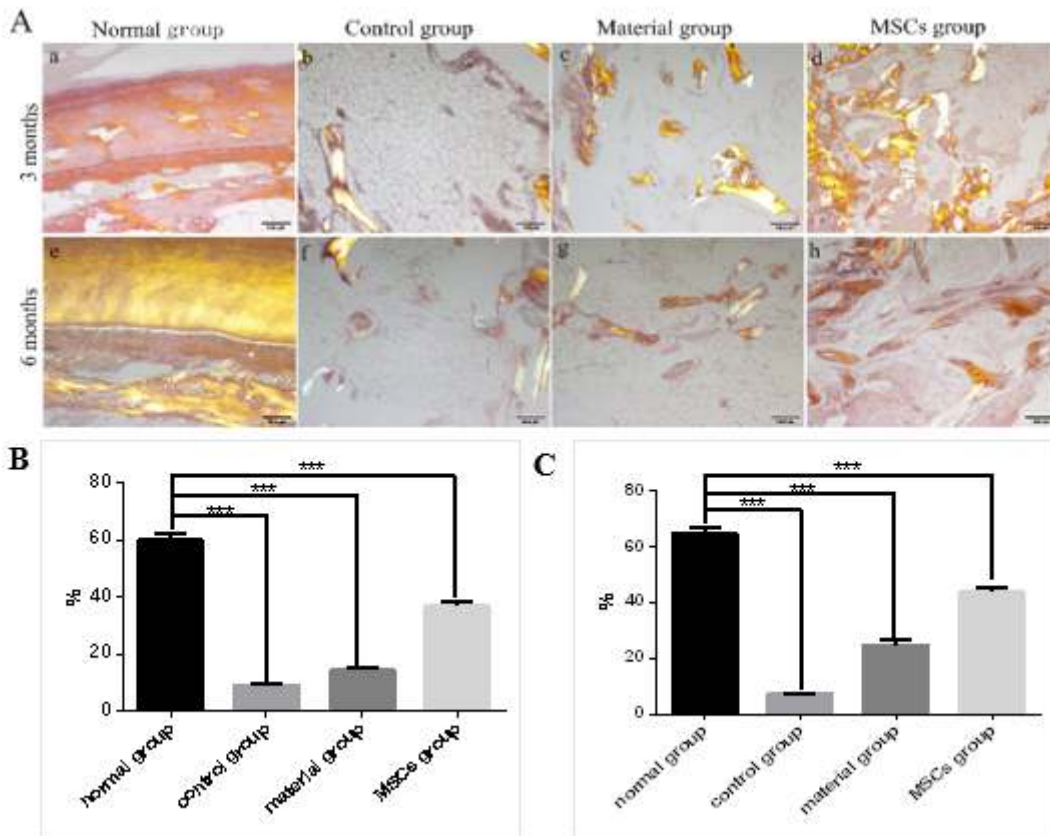


**Figure 6**

Sirius red staining results (40X). A a-d Sampling group 3 months after surgery; e-h Sampling group 6 months after surgery. a,e Normal group b,f Control group c, g Material group d, h MSCs group. Mark the area of the positive signal with a red arrow. B: The percentage of type 1 collagen in each group at 3 months after surgery. C: The percentage of type 1 collagen in each group at 6 months after surgery. All groups were compared with the Normal group, and the statistical difference was denoted by \*.

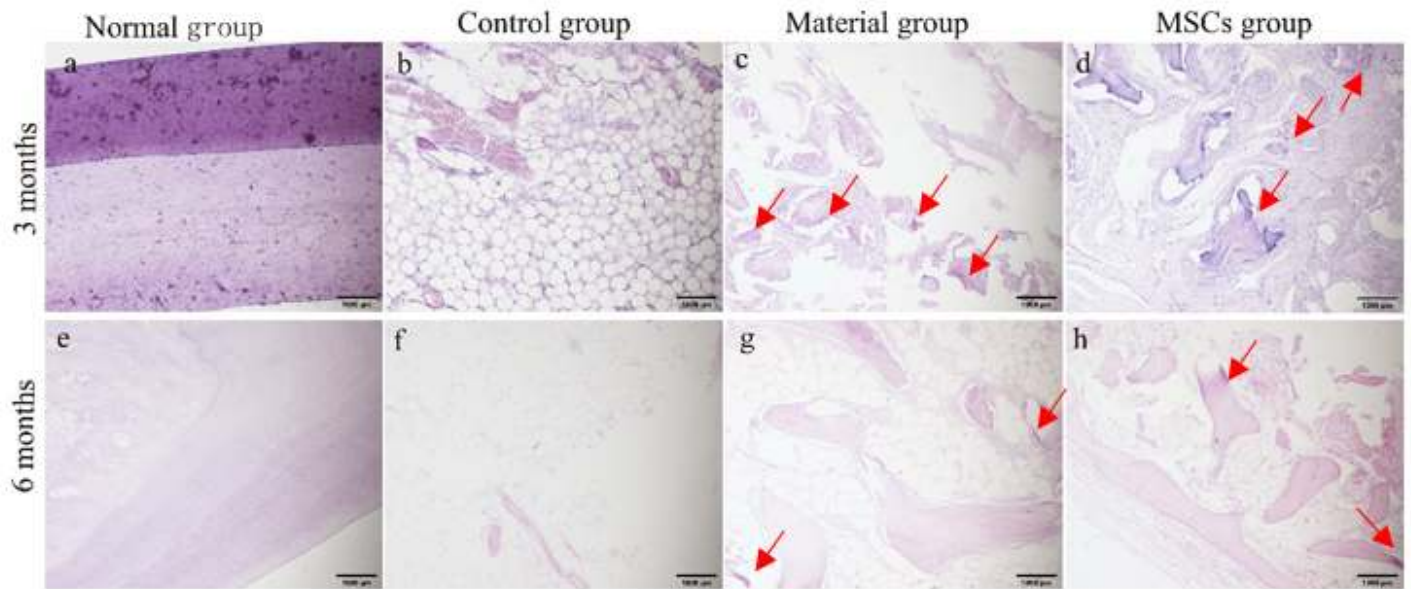


**Figure 7**

PAS staining results (100X). a-d Sampling group 3 months after surgery; e-h Sampling group 6 months after surgery. a,e Normal group b,f Control group c, g Material group d, h MSCs group. Mark the area of the positive signal with a red arrow.

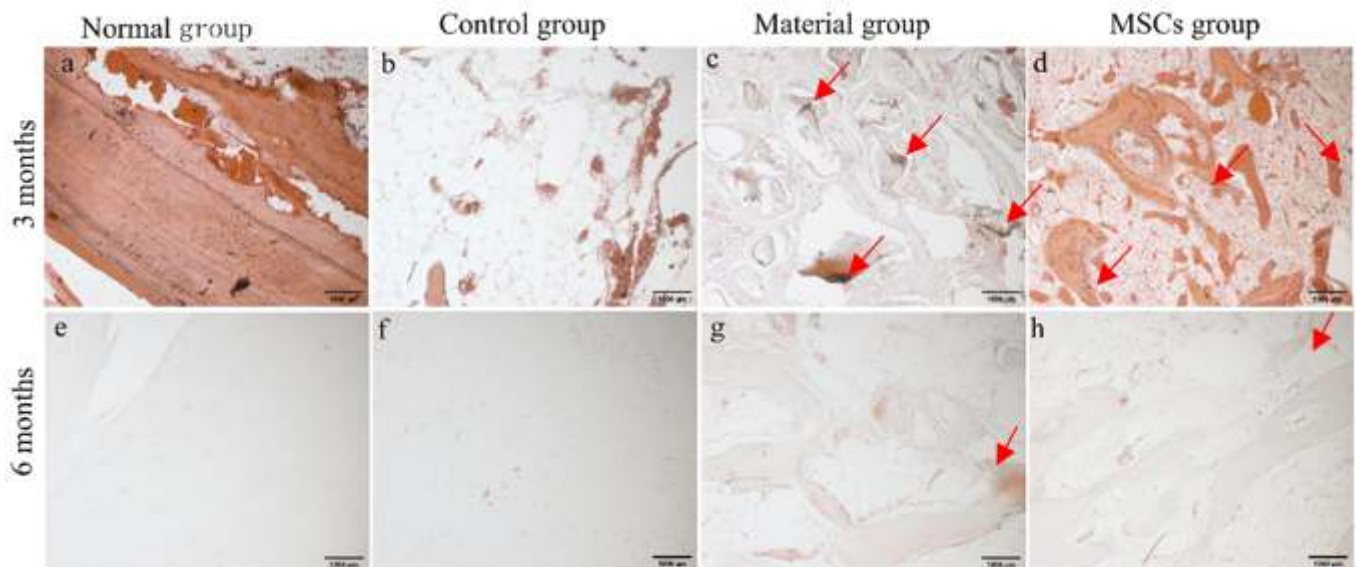


**Figure 8**

ALP staining results (100X).. a-d Sampling group 3 months after surgery; e-h Sampling group 6 months after surgery. a,e Normal group b,f Control group c, g Material group d, h MSCs group. Mark the area of the positive signal with a red arrow.

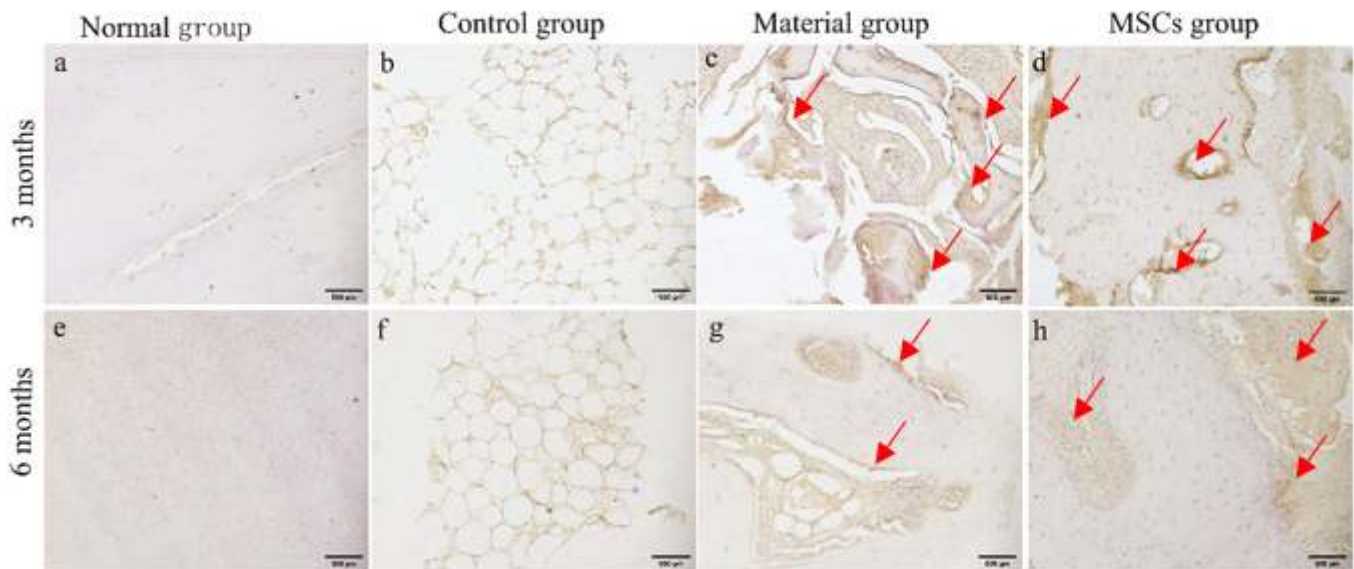


**Figure 9**

IHC results of MSCS2 (200X). a-d Sampling group 3 months after surgery; e-h Sampling group 6 months after surgery. a,e Normal group b,f Control group c, g Material group d, h MSCs group. Mark the area of the positive signal with a red arrow.



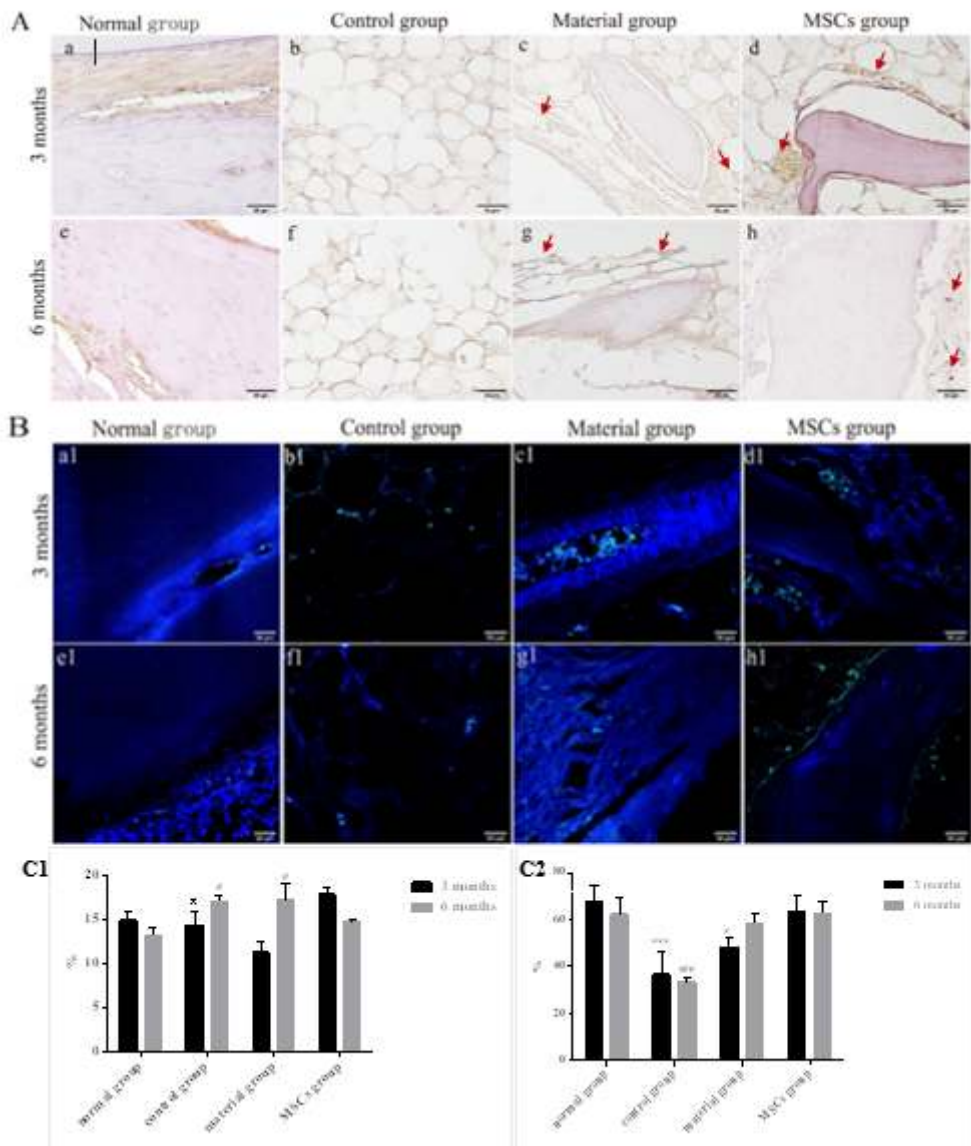


**Figure 10**

A TUNEL results (400X). B Ki67 results (400X). a-d&a1-d1 Sampling group 3 months after surgery; e-h&e1-h1 Sampling group 6 months after surgery. a,e&a1,e1 Normal group b,f&b1,f1 Control group c, g&c1,g1 Material group d, h&d1,h1 MSCs group. Mark the area of the positive signal with a red arrow. C1 Percentage of apoptotic cells in each group at 3 or 6 months. C2 Percentage of proliferative cells in each group at 3 or 6 months. Cells labeled in green represent cells that are proliferating. \* represents the statistical difference between each group and the normal group at 3 months. # represents the statistical difference between each group and the normal group at 3 months.